Crocus sativus tepals extract suppresses subcutaneous adipose tissue hypertrophy and improves systemic insulin sensitivity in mice on high-fat diet

Crocus sativus tepals extract suppresses subcutaneous adipose tissue hypertrophy and improves systemic insulin sensitivity in mice on high-fat diet

Biljana Bursać[1#], Luisa Bellachioma[2#], Ljupka Gligorovska[1], Mirna Jovanović[1], Ana Teofilović[1], Miloš Vratarić[1], Danijela Vojnović Milutinović[1], Alfonso Albacete[3], Purificación A. Martínez-Melgarejo[3], Camilla Morresi[2], Elisabetta Damiani[2], Tiziana Bacchetti[2]*, Ana Djordjevic[1]*

# Authors contributed equally to this work

Short title: *Crocus sativus* tepals dampen obesity and its complications

[1] Department of Biochemistry, Institute for Biological Research "Siniša Stanković"- National Institute of the Republic of Serbia, University of Belgrade, 142 Despot Stefan Blvd., 11000 Belgrade, Serbia

[2] Department of Life and Environmental Sciences, Marche Polytechnic University, Via Brecce Bianche, 60131 Ancona, Italy

[3] Centro de Edafología y Biología Aplicada del Segura, Agencia Estatal Consejo Superior de Investigaciones Científicas (CEBAS-CSIC), Department of Plant Nutrition, Campus Universitario de Espinardo, E-30100 Murcia, Spain

*Corresponding authors:

Tiziana Bacchetti, PhD, Department of Life and Environmental Sciences, Marche Polytechnic University, Via Brecce Bianche, 60131 Ancona, Italy

Phone: +39 071 2204968; E-mail: t.bacchetti@staff.univpm.it

Ana Djordjevic, PhD, Institute for Biological Research "Siniša Stanković"- National Institute of the Republic of Serbia, University of Belgrade, 142 Despot Stefan Blvd., 11000 Belgrade, Serbia

Phone: +381 11 207 83 03; Fax: +381 11 276 14 33; E-mail: djordjevica@ibiss.bg.ac.rs

Keywords: *Crocus sativus*; adipose tissue; obesity; insulin sensitivity; lipid metabolism

Abstract

Obesity is a pressing problem worldwide for which standard therapeutic strategies have limited effectiveness. The use of natural products seems to be a promising approach to alleviate obesity and its associated complications. The tepals of *Crocus sativus* plant, usually wasted in saffron production, are an unexplored source of bioactive compounds. Our aim was to elucidate the mechanisms of *Crocus sativus* (Cr) tepals extract in obesity by investigating its effects on adipocyte differentiation, visceral (VAT) and subcutaneous (SAT) adipose tissue hypertrophy, and lipid metabolism in an animal model of diet-induced obesity. To this end, mouse 3T3-F442A preadipocytes were treated with Cr tepals extract and the expression of adipocyte differentiation genes was determined. Caloric intake, body mass, triglycerides, systemic insulin sensitivity, histology, insulin signaling and lipid metabolism in VAT and SAT were analyzed in mice fed a 60% fat diet for 14 weeks and treated orally with Cr tepals extract during the last 5 weeks of the diet. We demonstrated for the first time that Cr tepals extract inhibits adipocyte differentiation *in vitro*. The animal model confirmed that oral treatment with Cr tepals extract results in weight loss, improved systemic insulin sensitivity, lower triglycerides, and improved lipid peroxidation. The suppressive effect of Cr tepals extract on adipocyte hypertrophy and inflammation was observed only in SAT, which, together with preserved SAT insulin signaling, most likely contributed to improved systemic insulin sensitivity. Our results suggest the functionality of SAT as a possible target for the treatment of obesity and its complications.

1. Introduction

The prevalence of obesity has escalated worldwide and is associated with increased morbidity, reduced quality of life, and high healthcare costs. Considering that routine therapeutic strategies – diet modifications and increased physical activity can be hard to follow through, while chemical drugs can have considerable side effects, the use of natural products is an attractive approach to reduce the discomfort of obesity treatment, thus increasing the treatment success rate, and attenuating the obesity-associated complications (1–3). Saffron, a spice derived from the stigmas of the flower *Crocus sativus*, has beneficial effects on insulin sensitization, as well as anti-inflammatory, antioxidant, lipid-lowering, and glucose-lowering activities (4–6). Previous studies have shown that crocin, a carotenoid found in the stigmas of *Crocus sativus,* attenuates insulin resistance associated with obesity and type 2 diabetes (7, 8), particularly due to its modulatory effects on inflammation and oxidative stress (9). Mashmoul *et al*. also demonstrated the anti-obesity effects of saffron by reducing body mass and food intake (10). Compared to other parts of the plant, the stigmas are considered to be the most valuable part of the *Crocus sativus* flower, which are used in the food, cosmetic and nutraceutical industry (11). However, Bellachioma *at al.* have recently shown that the tepals, wasted in saffron production, are also a rich source of bioactive

[1] **Abbreviations:** *Crocus sativus* (Cr); visceral adipose tissue (VAT); subcutaneous adipose tissue (SAT); high-fat diet (HFD); adipose tissue triglyceride lipase (ATGL); hormone-sensitive lipase (HSL); acetyl-CoA carboxylase (ACC); fatty acid synthase (FAS); lipoprotein lipase (LPL); fatty acid translocase (FAT/CD36); phosphoenolpyruvate carboxykinase (PEPCK); peroxisome proliferator-activated receptor γ (PPARγ); CCAAT/enhancer binding protein α (C/EBPα); sterol response element binding protein 1c (SREBP-1c); insulin receptor substrate 1 (IRS-1); protein kinase B (Akt); glycogen synthase kinase 3β (GSK3β)

components with hypoglycemic potential (12). In addition, an animal study has shown the protective effects of *Crocus sativus* (Cr) tepals extract against dyslipidemia, insulin resistance, and oxidative stress (13).

The main functions of white adipose tissue are to store excess energy in the form of triglycerides (lipogenesis) and to release it into the bloodstream in the form of free fatty acids (lipolysis). The key enzymes involved in lipolysis are adipose tissue triglyceride lipase (ATGL) and hormone-sensitive lipase (HSL), whereas lipid synthesis requires the action of enzymes involved in *de novo* lipogenesis (acetyl-CoA carboxylase, ACC and fatty acid synthase, FAS), lipid uptake (lipoprotein lipase, LPL and fatty acid translocase, FAT/CD36), fatty acid transport (fatty acid transport proteins, FATPs) and glyceroneogenesis (phosphoenolpyruvate carboxykinase, PEPCK) (14). The action of the corresponding proteins promotes the formation of a large intracellular triglyceride-containing droplet, which, together with the expression of perilipins and the secretion of specific hormones (adiponectin, leptin), is a hallmark of mature adipocytes (15). The main regulators of enlargement of adipocyte size (hypertrophy) and number (hyperplasia/adipogenesis) are peroxisome proliferator-activated receptor γ (PPARγ), CCAAT/enhancer binding protein α (C/EBPα), and sterol response element binding protein 1c (SREBP-1c), all of which influence adipocyte development through synergistic activation of key metabolic adipocyte genes (16, 17).

The distribution and expansion of different white adipose tissue depots are important for understanding the mechanisms underlying obesity and its associated diseases. The expansion of visceral adipose tissue (VAT) depot contributes to insulin resistance, inflammation, and

dyslipidemia (18), while the capacity of subcutaneous adipose tissue (SAT) to expand has been associated with improved insulin sensitivity and metabolic status (19). The ability of the SAT depot to store excess fat rather than fat accumulation in ectopic depots such as liver, muscle or heart has been recognized as one of the most important determinants of metabolically healthy obese (20). On the other hand, VAT expansion together with excessive ectopic lipid accumulation leads to the development of obesity-associated insulin resistance and inflammation (21). Inhibitory serine phosphorylation (Ser307) of insulin receptor substrate 1 (IRS-1) represents an early hallmark of insulin resistance, resulting in impaired ability of IRS-1 to activate downstream kinases such as protein kinase B (Akt) and glycogen synthase kinase 3β (GSK3β) (22). Given that hypertrophy and hyperplasia of adipocytes are characterized by the accumulation of macrophages in adipose tissue, chronic inflammation has been proposed as the main cause of obesity-induced insulin resistance in adipose tissue (23).

Although numerous studies indicate the hypolipidemic and hypoglycemic effects of *Crocus sativus* stigma extract due to its antioxidant and anti-inflammatory potential (24–26), the effect of Cr tepals extract on adipocyte development and metabolism has been poorly understood. Therefore, the aim of the present study is to clarify the possible mechanisms of Cr tepals extract in obesity by investigating the effects on adipose tissue development and VAT and SAT lipid metabolism. For this purpose, *in vivo* and *in vitro* studies were performed. The animal study was designed to determine the effects of 5-week Cr tepals extract treatment on caloric intake, body mass, and biochemical parameters, VAT and SAT mass and histology, adipose tissue insulin signaling pathway, and on the expression of genes

related to adipocyte differentiation and lipid metabolism in the VAT and SAT depots of mice on high-fat diet. In addition, mouse preadipocytes 3T3-F442A were insulin-stimulated and treated with Cr tepals extract to confirm the effect on the key determining genes involved in adipocyte differentiation.

2. Experimental Procedures

2.1 Plant material and extract preparation

Crocus sativus flowers were provided by a local farm Tesoro delle Api (Sant' Elpidio a Mare, FM, Italy) and were harvested between October and November 2021. *Crocus sativus* was cultivated without any chemical treatment. The tepals were manually separated from whole flowers and frozen at -20°C before being lyophilized in a freeze dryer (LYOQUEST-55, Seneco, Italy). The freeze-dried samples were stored at -20°C (12). The tepals extract was obtained by placing the lyophilized tepals (2 g) in 100 mL of ethanol/water 80/20 (v/v) under magnetic stirring for 24 h at 4°C in the dark (27). The hydroalcoholic extract of tepals was subsequently centrifuged twice at 2000 rpm for 10 min. The pellets were recovered, and this extraction procedure was repeated two more times. The supernatants were pooled and concentrated by rotary evaporation (Heidolph Laborota 4000 efficient; Heidolph Instruments GmbH & Co, Schwabach, Germany) and then dried in a SpeedVac (Hetovac VR-1, HETO Lab Equipment, Gydevang 17-19, 3450, ALLERØD, Denmark). These tepals extracts were stored at -20°C until use. Before administration, the dry extract was dissolved in phosphate-buffered saline (PBS) and the suspension was administered to cell culture at doses of 25 or 100 μg/mL, or administered daily to mice at a dose of 250 mg/kg bodyweight for 5 weeks by

oral gavage (27). The preparation and the dose of tepals extract used were selected according to previous studies on animal models (28–31). Selected dose given to the animals extrapolates to the human equivalent dose (HED) through normalization to body surface area and is calculated according to Reagan-Shaw et al. (32). The calculation results in a HED of 20 mg/kg bodyweight, which is about 10 times lower compared to the values reported as the safe dose for humans of several “herbal medicines” (33).

2.2 Metabolomic profiling

Tepals extracts were filtered through 13 mm diameter Millex filters with 0.22 µm pore size nylon membrane (Millipore, Bedford, MA, USA). Ten microliters of filtered extract were injected using an ultra-high performance liquid chromatography device (U-HPLC, Accela Series, ThermoFisher Scientific, Waltham, MA, USA) coupled to a high-resolution mass spectrometer (HRMS, Exactive, ThermoFisher Scientific, Waltham, MA, USA) consisting of an Orbitrap detector and using a heated electrospray ionization (HESI) interface. Data processing was carried out through the Xcalibur software (version 4.3, ThermoFisher Scientific, Waltham, MA, USA); the XCMS metabolomics platform (Scripps Center for Metabolomics and Mass Spectrometry, La Jolla, CA, USA) and the KEGG, PUBCHEM and PHE-NOL-EXPLORER chemical databases, among others. For fine-tuning the analysis method, the molecular formulas of the compounds were searched in the PUBCHEM platform and entered in the Qual Browser package of the Xcalibur software, where mass/charge (m/z) ratios of each metabolite were identified in the negative mode, adjusting a mass tolerance of ≤2 ppm in the Processing Setup Package. Additionally, correlations between compounds of the same metabolic pathway and the LogP coefficient were used to accurately identify these

metabolites. Compounds identified in *Crocus sativus* tepals extracts through U-HPLC-HRMS technique are shown in the Supplementary table (S1).

2.3 Cell culture

Mouse preadipocytes 3T3-F442A (00070654, ATCC, USA) (passage 9) were grown for propagation in Dulbecco′s Modified Eagle′s Medium (DMEM) (DMEM-HXA, Capricorn, Germany), supplemented with 10% fetal bovine serum (FBS-11A, Capricorn, Germany) and 1% Penicillin/Streptomycin solution (PS-B, Capricorn, Germany), while the differentiation medium was additionally supplemented with 10 μg/mL of insulin (I0516, Sigma, Germany). The cells were grown at 37°C in a humidified 5% CO_2 atmosphere.

The cells were seeded into 60x15 mm tissue culture dishes (LUX 5220, Miles Laboratories Inc., USA), at a density 425,000 cells/dish. Once 90% confluent, differentiation was initiated with appropriate medium, and the medium was changed every 2–3 days. The cells were differentiated for 14 days. The cells were treated with 25 or 100 μg/mL of Cr tepals extract for 5 days (days 9^{th} to 14^{th} of differentiation), or during the whole 14 days of differentiation.

2.4 Animals and experimental design

Male C57BL/6J mice (2.5 months old) bred in our laboratory were randomly divided into three groups (at least 9 animals in each group): control group (C), high-fat diet (HFD) group, and high-fat diet and Cr tepals extract (HFD+Cr) group. Group C received a control diet (rodent diet with 10 kcal% fat, D12450J, Research diets, New Brunswick, USA), while the HFD and HFD+Cr groups received a high-fat diet (rodent diet with 60 kcal% fat, D12492, Research diets, New Brunswick, USA) during the 14-week treatment. Allocation of the animals to the experimental groups was performed by appropriate randomization method in

order to ensure blinding and reduction of systematic differences in the characteristics of animals assigned to experimental groups. After 9 weeks, the HFD+Cr group started receiving a dose of 250 mg/kg bodyweight Cr tepals extract dissolved in PBS, while the control and HFD groups received PBS without Cr tepals extract. All animals received these solutions orally by gavage once daily for the last 5 weeks of treatment and had *ad libitum* access to food and water throughout the 14 weeks of treatment. During the experiment, 2 animals at a time were housed per cage, separated by a perforated transparent acrylic partition so that they were not socially isolated and could communicate with each other, but individual food intake could be monitored. Animals were housed under standard conditions at 22±2°C with a 12-h light-dark cycle and constant humidity. Food intake per animal was recorded daily, and daily caloric intake was calculated as follows: for control group [mass of food ingested per day (g) × 3.85 kcal/g], whereas for the mice fed a high-fat diet [mass of food ingested per day (g) × 5.24 kcal/g]. Body mass was recorded weekly. All animal procedures were in compliance with the EEC Directive 2010/63/EU on the protection of animals used for experimental and other scientific purposes and were approved by the Ethical Committee for the Use of Laboratory Animals of the Ministry of Agriculture, Forestry and Water Economy of the Republic of Serbia (No. 323-07-02390-2022-05 from 28.02.2022).

2.5 Serum and tissue preparation and determination of blood triglycerides

After fasting for 4 h, the animals were killed by rapid decapitation, and the trunk blood was collected. Blood triglycerides were measured onsite by Accutrend® strips (F. Hoffmann-La Roche AG, Basel, Switzerland). The serum was prepared by separation following low-speed

centrifugation (2000xg for 10 min) after incubation at room temperature for 30 minutes. Serum was stored at -70°C for further analyses.

Immediately after decapitation, the depots of VAT (epididymal, retroperitoneal, mesenteric, and perirenal) and SAT (anterior and posterior) were carefully collected and weighed. Adiposity index (AI) was calculated using the following formula: AI = [mass of total VAT depots (epididymal, retroperitoneal, mesenteric, and perirenal)/total body mass)]×100 (34). For the VAT histological and molecular analyses, the epididymal depot (eVAT) was selected because it is the primary storage depot in C57BL/6J mice that initially increases with dietary obesity (35). On the other hand, the posterior inguinal depot (iSAT) was chosen for the histological and molecular analyses of SAT because it has been shown that this depot plays a more active role in influencing insulin sensitivity in the context of obesity (36, 37). Portions of tissue for molecular analyses were frozen in liquid nitrogen and stored at -70°C for later analyses, while those for histological analyses were fixed in 4% paraformaldehyde.

2.6 Systemic insulin sensitivity parameters

Serum insulin concentrations were measured using the rat/mouse insulin ELISA kit (#EZRMI-13K) according to the manufacturer's instructions (EMD Millipore Corporation, St. Louis, Missouri, USA). The sensitivity of the assay was 0.1 ng/mL (17.5 pM) insulin with a sample size of 10 µL, and the intra-assay coefficient of variation was 1.92%.

Systemic insulin sensitivity was estimated by the homeostasis model assessment (HOMA) index and glucose tolerance was assessed using the intraperitoneal glucose tolerance test (ipGTT). The HOMA index was calculated using fasting plasma insulin and glucose concentrations according to the following formula: [insulin (mIU/L) x glucose

(mmol/L)]/22.5. Glucose tolerance was determined by ipGTT, which was performed 3 days before the end of the experiment. Mice were fasted for 4 h, and glucose was administered intraperitoneally (2 g/kg). Glucose concentration was measured with Accu-Chek® strips (F. Hoffmann-La Roche AG, Basel, Switzerland) from tail vein blood, drawn at 0, 15, 30, 60, 90, 120, and 150 min after glucose injection. The area under the concentration vs. time curve (AUC glucose 0-150 min, mmol/L *vs.* min) was calculated by the trapezoidal rule.

2.7 Measurement of lipid peroxidation level

Lipid peroxidation level was determined by thiobarbituric acid reactive substances (TBARS) assay kit (Merck, Darmstadt, Germany) in the serum according to the manufacturer's instructions. Readings were taken spectrophotometrically at 532 nm using the Multiskan Spectrum (Thermo Electron Corporation, Waltham, MA, United States), and the TBARS concentration in the samples was extrapolated from the standard curve and expressed in nmol/mL.

2.8 Histological and morphometric analysis of adipose tissue depots

For histological analysis, portions of the eVAT and iSAT depots were removed and fixed in 4% paraformaldehyde for 24 h, dehydrated in an ethanol gradient, cleared in xylene, and embedded in paraffin. Both eVAT and iSAT blocks were sectioned at 10-μm thickness and stained with hematoxylin-eosin. Images for analysis were acquired with a Leitz DMRB light microscope equipped with a Leica MC190 HD camera and Leica Application Suite (LAS) 4.11.0 software (Leica Microsystems, Wetzlar, Germany) at 20× magnification. Adipocyte area and diameter were determined using ImageJ plugin Adiposoft 1.16 software (38), using 100 adipocytes per section, three sections per animal, and five animals per group.

Crown-like structures (CLS) were detected using hematoxylin-eosin staining (39) and their density in adipose tissue depots was calculated as previously described (40). For each animal group, CLS density per 1500 adipocytes was determined using ImageJ plugin Adiposoft 1.16 software (100 adipocytes per section, three sections per animal, and five animals per group).

2.9 Adipocytes and adipose tissue RNA extraction, reverse transcription and real-time PCR

Total RNA was extracted from the 3T3-F442A following treatment, or mice eVAT and iSAT depots using TRI reagent solution (AM9738, Thermo Fisher Scientific, USA) according to the manufacturer's instructions. RNA concentrations were quantified on NanoPhotometer N60 (Implen, Munich, Germany) by reading the optical density at 260 nm, while the quality and integrity of RNA was confirmed on 2% agarose gel. Reverse transcription was performed using a High-Capacity cDNA Reverse Transcription Kit (Applied Biosystems, USA), according to manufacturer's instructions and the cDNAs were stored at −70°C until use.

To determine mRNA expression levels of genes of interest, real-time PCR was performed using Advanced Universal SYBR Green Supermix (Bio-Rad Laboratories, USA) and specific primers (Applied Biosystems, USA): *Hsl*: F 5′-GGCTCA CAG TTA CCA TCT CAC C-3′, R 5′-GAG TAC CTT GCTGTC CTG TCC-3′; *Lpl*: F 5′-TTC CAG CCA GGA TGC AACA-3′, R 5′-GGT CCA CGT CTC CGA GTC C-3′; *Atgl*: F 5′-AAC ACC AGC ATC CAG TTCAA-3′, R 5′-GGT TCA GTA GGC CAT TCC TC-3′; *Fasn*: F 5′-TTG CTG GCA CTA CAGAAT GC-3′, R 5′-AAC AGC CTC AGA GCG ACA AT-3′; *Pepck*: F 5′-AAC TGT TGG CTG GCT CTC-3′, R 5′-GAA CCT GGCGTT GAA TGC-3′; *Adipo* F 5'-GCA CTG GCA AGT TCT ACT GCAA-3', R 5'-GTA GGT GAA GAG AAC GGC CTTGT-3'; *C/EBPα*: F 5'-CAA GAA CAG CAA CGA GTA CCG-3', R 5'-GTC ACT GGT CAA CTC

CAG CAC-3′, *Pparg*: F 5'-GTG CCA GTT TCG ATC CGT AGA-3', R 5'-GGC CAG CAT CGT GTA GAT GA-3'. Normalization of cDNA was performed using *Hprt*, as endogenous control (*Hprt*: F 5′-TCC TCC TCA GAC CGC TTT T-3′, R 5′-CCT GGT TCA TCA TCG CTA ATC-3′). All reactions were performed in duplicate in 20 μL volume containing 20 ng of cDNA template using Quant Studio™ Real-Time PCR System (Applied Biosystems, USA). Thermal cycling conditions were 2 min incubation at 50°C, 10 min at 95°C, followed by 45 cycles of 95°C for 15 s and 60°C for 60 s. In the mice eVAT and iSAT, the same cDNA sample was used as calibrator on each plate. Melting curve analyses were performed to confirm the formation of a single PCR product. Relative quantification of gene expression was performed using the comparative $2^{-\Delta\Delta Ct}$ method (41), where ΔCt represents the difference between Ct value of gene of interest and the endogenous control. The results were analyzed by Quant Studio Design and Analysis Software v1.4.0 (Applied Biosystems, USA) with a confidence level of 95% ($p \leq 0.05$).

2.10 Preparation of total protein fraction from adipose tissue depots

Total protein fraction of the eVAT and iSAT depots was prepared with TRIzol protocol, according to the manufacturer's instruction. After RNA precipitation, ethanol was added in the remaining organic phase, followed by centrifugation at 2000xg for 5 min at 4°C. Protein fraction was precipitated from phenol-ethanol supernatant using acetone and by centrifugation at 12000xg for 10 min at 4°C. The protein pellets were redissolved in 0.3 M guanidine hydrochloride in 95% ethanol with 2.5% glycerol, followed by sonication on ice and washing in the same buffer. After protein pelleting by centrifugation at 8000xg for 5 min

at 4°C, pellets were dissolved in the lysis buffer containing 2.5 mM Tris–HCl pH 6.8, 2% SDS, 10% glycerol and 50 mM DTT. Samples were stored at −70°C for further analysis.

2.11 Western blot analysis

Protein concentration was determined by the Lowry method (42) using bovine serum albumin (BSA) as a standard. The samples were boiled in 2x Laemmli buffer for 5 min and 40 µg of proteins were subjected to electrophoresis on 7.5% or 10% sodium dodecyl sulfate-polyacrylamide gels (SDS-PAGE). The proteins were transferred from gels to polyvinylidene difluoride (PVDF) membranes (Immobilon-FL, Millipore, USA), blocked for 1 h with 5% non-fat milk or 2% BSA and incubated overnight at 4°C with specific primary antibodies: anti-phospho-IRS1-Ser307 (1:500, Abcam, Cambridge, UK, ab5599), anti-IRS-1 (1:1000, FineTest , FNab10261), anti-phospho-GSK-3β-Ser9 (1:1000, Santa Cruz Biotechnology, sc-373800), anti-GSK-3α/β (1:1000, Santa Cruz Biotechnology, sc-7291), anti-phospho-AKT1/2/3-Thr308 (1:500, Santa Cruz Biotechnology, sc-16646-R), anti-AKT1/2/3 (1:500, Santa Cruz Biotechnology, sc-81434), anti-SREBP1c (1:500, Santa Cruz Biotechnology, sc-366), anti-PPARɣ (1:1000, Santa Cruz Biotechnology, sc-7273), anti-CD36 (1:500, Santa Cruz Biotechnology, sc-7309), anti-FATP4 (1:500, Santa Cruz Biotechnology, sc-393309), anti-perilipin-2/ADFP (1:1000, Novus Biologicals, NB110-40877). Anti-calnexin antibody (1:2000, Abcam, ab2259) was used as controls of equal loading of total protein fractions in all the samples (43). Membranes were extensively washed in PBS containing 0.1% Tween-20 and incubated for 90 min with corresponding mouse (1:30000, Abcam, ab97046) or rabbit (1:20000, Abcam, ab6721) HRP-conjugated secondary antibodies. The immunoreactive protein bands were detected by chemiluminescent (ECL) method using iBright CL1500

(Thermo Fisher Scientific, USA) and quantitative analysis was performed by iBright software.

2.12 Statistical analyses

The data collected from animal model are presented as means ± SEM. All data were tested for normality by Shapiro–Wilk test. Unless otherwise specified, normally distributed data were analyzed by one-way ANOVA followed by *post hoc* Tukey test. Data with deviation from normal distribution were analyzed by non-parametric Kruskal–Wallis *H* test followed by *post hoc* Dunn's test. The data collected from cell culture are presented as means ± SD. All data were tested for normality by D'Agostino&Pearson omnibus normality test. The treatments were compared to untreated controls. Normally distributed data were analyzed by unpaired t test with Welch's correction. The data without normal distribution were analyzed by Mann-Whitney *U* test.

The differences between groups were considered significant at $P<0.05$. Statistical analyses were performed using GraphPad Prism 8 software (San Diego, USA).

3. Results

3.1 Crocus tepal extract polyphenolic profile

U-HPLC-HRMS analysis of the hydroalcoholic *Crocus sativus* tepals extract used in this study revealed a total of 131 phenolic compounds that included flavonoids (i.e., anthocyanins, dihydrochalcones, flavonols, isoflavonoids), phenolic acids (hydroxybenzoic acids, hydroxycinnamic acids, hydroxyphenypropanoic acids), stilbenes and other

polyphenols. The comprehensive list of all the phenolic compounds annotated is reported in the Supplementary Table S1, together with their relative abundance. The polyphenolic profile of the hydroalcoholic tepals extract is in accordance with that found in other studies (12, 44, 45).

3.2 Caloric intake and morphological parameters of animals

The body mass of the animals did not differ significantly at the beginning of the experiment (**Table 1**). As expected, all mice on high-fat diet had increased caloric intake, eVAT and iSAT depot masses ($P<0.001$), and AI ($P<0.01$) as compared with the control group, regardless of Cr tepals extract treatment (**Table 1**). After 9 weeks on a high-fat diet and before oral administration of the extract, both groups of mice on a high-fat diet had an increased body mass ($P<0.05$, **Table 1**). Total body mass at the end of the experiment was also significantly higher in the group receiving a high-fat diet compared with the control group ($P<0.001$), while this increment was lower after Cr tepals extract treatment ($P<0.01$). Hence, administration of Cr tepals extract significantly decreased total body mass, as well as iSAT depot mass compared with the HFD group ($P<0.05$, **Table 1**).

3.3 Histological and morphometric analysis of eVAT and iSAT depots

To determine the effects of a high-fat diet and Cr tepals extract treatment on the morphology of the different adipose tissue depots, we performed histological and morphometric analysis of the eVAT and iSAT depots. Representative sections of the eVAT and iSAT depots are shown in **Figure 1.A1** and **B1**, respectively. Morphometric analysis showed that in the eVAT depot, both adipocyte diameter and area were significantly increased in both groups on high-fat diet compared with the control group, regardless of Cr tepals extract ($P<0.001$, **Figure**

1.A2 and **A3**). On the other hand, regarding the iSAT depot, adipocyte diameter and area were increased relative to control group only when mice were fed a high-fat diet without administration of Cr tepals extract (P<0.001, **Figure 1.B2** and **B3**). In this depot, treatment with Cr tepals extract significantly reduced both adipocyte area and cell diameter compared with animals receiving a high-fat diet alone (P<0.001, **Figure 1.B2** and **B3**). This differential effect of high-fat diet and Cr tepals extract on the morphology of eVAT and iSAT depots was further confirmed by analysing the size distribution of adipocytes (**Figure 1.A4** and **B4**) and the density of the CLS (**Figure 1.A1** and **B1**). As shown in **Figure 1.A4**, all animals on HFD regardles of the Cr treatment, had a significantly lower proportion of small adipocytes (<50 µm, P<0.001) in the eVAT, and a higher proportion of large (70-89 µm, P<0.001) and very large adipocytes (>90 µm, P<0.001). In the iSAT depot the proportion of small adipocytes (<50 µm) was decreased relative to the control group when mice were fed with HFD (P<0.001) and with HFD and Cr tepals extract (P<0.01, **Figure 1.B4**). Also, Cr tepals extract increased the freqency of small adipocytes in comparison to the HFD alone (P<0.001). The proportion of large adipocytes (70-89 µm) was increased in HFD group (P<0.001) and with lower significance in Cr tepals extract treated group (P<0.05). Thus, the proportion of large adipocytes was significantly reduced after Cr tepals extract administration in comparison to mice on a high-fat diet (P<0.001). The iSAT depot had a higher proportion of very large adipocytes (>90 µm) after a high-fat diet without Cr tepals extract administration compared with control animals (P<0.01), resulting in a higher mean adipocyte size only in this group of animals (**Figure 1.B2** and **B3**). As shown in **Figure 1.A1** and **B1**, the number of CLS in the eVAT of all animals with HFD was increased regardless of Cr

treatment, whereas administration of Cr-Tepal extract reduced the number of CLS in the iSAT to the control level.

3.4 Systemic insulin sensitivity parameters, triglycerides and TBARS level

Glucose homeostasis was estimated from fasted glucose and insulin serum levels, HOMA index was used for the estimation of insulin sensitivity, while glucose tolerance was estimated through ipGTT-AUC values. As shown in **Table 2** and **Figure 2**, Cr tepals extract administration reverted the increase in glucose homeostasis and insulin sensitivity parameters induced by the high-fat diet. Only mice fed with high-fat diet without Cr tepals extract treatment showed increased fasting glucose level (P<0.001), insulin level (P<0.05), HOMA index (P<0.01) and ipGTT AUC value (P<0.001) compared with the control group (**Table 2**). In addition, the HFD group showed worse profiles for ipGTT AUC levels compared with control animals (for T0: P<0.001; for T15: P<0.01; for T30: P<0.001; for T60: P<0.01; for T90: P<0.05; for T150: P<0.01, **Figure 2**). However, after administration of Cr tepals extract, AUC value was significantly lower in comparison to high-fat diet alone (P<0.01, **Table 2**) and the response to a glucose load was significantly improved after 30 min in this group of animals compared with the HFD group (P<0.05). As expected, the ameliorating effect of Cr tepals extract against dyslipidemia and oxidative stress was also confirmed. Namely, administration of Cr tepals extract significantly decreased blood triglyceride levels compared with the control group (P<0.05, **Table 2**). In addition, Cr tepals extract treatment significantly decreased the amount of TBARS, which is a direct measure of lipid peroxidation and a marker of oxidative stress, compared with both the control group and the high-fat diet group (P<0.01, **Table 2**).

3.5 Insulin signaling pathway in the eVAT and iSAT depots

The effect of the high-fat diet and Cr tepals extract on the eVAT and iSAT insulin signaling pathways was estimated from the protein levels of IRS-1 with its inhibitory phosphorylation on Ser307, Akt with its stimulatory phosphorylation on Thr308, and GSK3β with its stimulatory phosphorylation on Ser9. As shown in **Figure 3.A1**, we observed impaired local insulin sensitivity in the eVAT depot, as the pIRS1^{Ser307}/IRS1 ratio was significantly increased in both high-fat diet groups compared with the control group, regardless of Cr tepals extract treatment (P<0.05, **Figure 3.A1**). However, this ratio remained unchanged in the iSAT depot (**Figure 3.B1**), suggesting that the disruption of the insulin signaling pathway after a high-fat diet occurs only in the eVAT depot. This was consistent with the changes in the analyzed kinases involved in the insulin signaling pathway. Both the pAkt^{Thr308}/Akt ratio and the pGSK3β^{Ser9}/GSK3α/β ratio were decreased in the eVAT depot after a high-fat diet, but only in the absence of Cr tepals extract administration (P<0.05, **Figure 3.A2** and **3.A3**). On the other hand, Cr tepals extract administration in the iSAT depot increased pAkt^{Thr308}/Akt ratio in the group receiving high-fat diet and Cr tepals extract compared to the group receiving only high-fat diet (P<0.05, **Figure 3.B2**).

3.6 In vitro differentiation of adipocytes

After the observed effects on histological traits and insulin signaling in iSAT depot with Cr tepals extract treatment, we wanted to see if the tepals extract affects the adipocyte cells' differentiation directly. Apart from pharmacokinetics, which has to be considered for drugs and phytochemicals, an important aspect of mechanistic studies is the question of whether the effect in question occurs through a direct interaction of the phytochemical with (fat) cells

and tissue or whether the target is another cell type, of other tissue and organ, that ultimately affects the adipose tissue as well. For this reason, an *in vitro* study was conducted to determine whether the extracts active ingredients have a direct effect on adipocytes. To determine this, we treated mouse adipocytes 3T3-F442A cells, stimulated to differentiate, with 25 or 100 μg/mL of Cr tepals extract for 5 days (day 9^{th} to 14^{th} of differentiation), or during the whole 14 days of differentiation. As shown in **Figure 4**, both treatment duration and applied concentrations significantly reduced the expression levels of key transcription factors for adipocyte differentiation and maturation, by at least 50% compared to the untreated control group (25 μg/mL: $P<0.001$, 100 μg/mL: $P< 0.05$ for *Pparg*; 25 μg/mL: $P<0.05$, 100 μg/mL $P<0.001$ for *Adipo*; both treatments: $P<0.001$ for *Cebpa*).

3.7 Markers of adipose tissue lipid metabolism

To evaluate the effects of the high-fat diet and Cr tepals extract treatment on eVAT and iSAT adipogenesis, lipid metabolism, and fatty acid transport, we analyzed protein levels of SREBP1c, PPARγ, and perilipin-2 (**Figure 5.A1** and **Figure 5.B1**, respectively), CD36 and FATP4 (**Figure 6.A1** and **Figure 6.B1**) and mRNA levels of genes involved in lipolysis and adipo/lipogenesis (**Figure 7.A1**, **A2** and **Figure 7.B1, B2**). As expected, the high-fat diet without Cr tepals extract administration led to an increase in protein concentrations of SREBP1c ($P<0.05$) and perilipin-2 ($P<0.001$), but only in the eVAT depot (**Figures 5.A1**), whereas PPARγ protein levels remained unchanged in both depots in all groups (**Figures 5.A1** and **B1**). Moreover, the applied treatments did not affect the protein levels of the fatty acid transporters CD36 and FATP4 in the eVAT depot (**Figure 6.A1**), whereas in the iSAT,

the protein level of CD36 decreased only in the HFD+Cr group compared to the HFD group (P<0.05, **Figure 6.B1**).

As shown in **Figures 7.A1** and **7.A2**, the mRNA levels of genes encoding the major lipolytic enzymes (*Hsl*, *Lpl* and *Atgl)* and the relative expression of markers of adipo/lipogenesis (*Adipo*, and *C/EBPα*) in the eVAT depot were decreased in HFD group (for *Hsl*: P<0.001; for *Lpl*, *Atgl* and *Cebpa*: P<0.01; for *Adipo*: P<0.05) and in the group treated with Cr tepals extract as compared with the control group (for *Hsl* and *Lpl*: P<0.001; for *Atgl*, *Adipo* and *Cebpa*: P<0.01). Moreover, the expression of the gene encoding the lipogenic enzyme *Fasn* was lower in the eVAT depot only after Cr tepals extract treatment as compared with control (P<0.001) and high-fat group (P<0.01). Expression of the gene encoding *Pepck*, another lipogenic enzyme, was decreased in the eVAT depot in both high-fat diet group (P<0.001) and Cr tepals extract treated group as compared with the control group (P<0.05), but it was increased after Cr tepals extract administration compared with the high-fat diet group (P<0.05, **Figure 7.A2**). In the iSAT depot, treatment with Cr tepals extract decreased the expression of *Hsl* and *Atgl* coding genes compared to the control group (**Figure 7.B1**, for *Hsl*: P<0.05; for *Atgl*: P<0.01), and also the mRNA level of *Hsl* compared with the high-fat diet group (P<0.001). The expression level of *Lpl* was lower in the high-fat diet group only after Cr tepals extract administration (P<0.01, **Figure 7.B1**). Consistent with the changes in eVAT, the mRNA level of *Fasn* in iSAT was also decreased only after Cr tepals extract treatment compared with the control (P<0.001) and high-fat group (P<0.01, **Figure 7.B2**). The expression of *Pepck*, *Adipo*, and *Cebpa* was decreased in the iSAT depot after a high-fat diet (for *Pepck*: P<0.01; for *Adipo* and *Cebpa*: P<0.001), as well as after Cr tepals extract

treatment compared with the control group (for *Pepck* and *Cebpa*: $P<0.001$; for *Adipo*: $P<0.01$, **Figure 7.B2**).

4. Discussion

Numerous studies to date have confirmed the anti-obesity potential of *Crocus sativus* stigmas, while the role of *Crocus sativus* tepals as a source of bioactive compounds remains poorly understood. In the present study, we demonstrated for the first time that *Crocus sativus* tepals have an anti-adipogenic effect on 3T3-F442A preadipocytes by inhibiting their differentiation, and also in obese mice on a high-fat diet, because of the suppressive effect on hypertrophy of SAT, but not of VAT adipocytes. In addition, our results confirmed that 5 weeks of oral treatment with *Crocus sativus* tepals extract in mice fed a high-fat diet resulted in weight loss, improved systemic insulin sensitivity, lower triglyceride levels, and improved lipid peroxidation.

The results confirmed that all animals fed a HFD for 14 weeks developed obesity, as caloric intake, adiposity index, total body mass, and the mass of the two adipose tissue depots studied increased independently of Cr tepals extract treatment. However, the treatment with Cr tepals extract resulted in the reduction of the body mass and iSAT mass, relative to the high-fat diet control group. These results are in line with the work by Mashmoul *et al*., where saffron and its bioactive compound crocin had a significant effect in reducing body mass, total fat mass, and the mass ratio of epididymal fat to total body fat in an obesity animal model (46). Mohaqiq *et al.* demonstrated that treatments with both saffron stigma and petal extracts resulted in a decrease in lipid peroxidation, weight loss, and improvement in dyslipidemia in

rats fed a high-fat diet (47). Oral administration of Cr tepals extract resulted in a decrease in systemic TBARS levels, one of the end products of lipid peroxidation. This is coherent with the well-known antioxidant activity of polyphenols found in abundance in Cr tepals extract (48).

As a particularly interesting result, Cr tepals extract reduced the effect of the high-fat diet on iSAT adipocyte size as adipocyte area and cell diameter in this depot were significantly reduced following the Cr tepals extract treatment, compared with control animals on a high-fat diet. As previously suggested (49, 50), reducing the size of subcutaneous fat cells may play a more important role in improving insulin sensitivity than reducing subcutaneous fat mass per se. Adipose tissue metabolism depends on the influx of free fatty acids from the bloodstream, and we observed that in the iSAT, CD36 protein levels were decreased after the administration of Cr tepals extract. CD36 is a key factor in the uptake of fatty acids and subsequent storage of triglycerides in adipocytes, and mice lacking CD36 have reduced adiposity and improved insulin resistance (51). Previous data suggest that CD36 expression is more sensitive to metabolic perturbations in SAT compared with VAT (52). The decrease in the size of iSAT adipocytes and presumably decreased capacity for fatty acid uptake was accompanied by decreased lipolytic capacity in response to Cr tepals extract treatment, concluded by reduced mRNA levels of the major lipolytic enzymes *Hsl*, *Atgl*, and *Lpl*.

However, the Cr tepals extract effect on adipocyte size reduction was not observed in eVAT, where morphometric analysis showed that the proportion of large adipocytes was significantly increased in the eVAT of both groups on high-fat diet, regardless of the effect of Cr tepals extract. On the other hand, the increased expression of lipogenic factors,

SREBP1c, and perilipin-2 was present only in the eVAT depot of the high-fat diet control group but not in the Cr tepals extract treated group. Nonetheless, none of the applied treatments affected the fatty acid transporters FATP4 and CD36 in eVAT.

Obesity is associated with impaired adipose tissue function. Beyond adipocyte hypertrophy and impaired lipolysis, this impaired tissue is characterized by inflammation, and chronic inflammation caused by obesity is thought to be an important mediator of systemic insulin resistance (53). The increased inflammation in the adipose tissue is characterized histologically by the presence of CLS. In the present study, we demonstrated that increased adipocyte hypertrophy in the eVAT depot of mice on a high-fat diet was associated with a high degree of inflammation, as indicated by the high number of CLS structures. VAT hypertrophy is often associated with dyslipidemia and a pro-inflammatory state that may be related to systemic insulin resistance (54). On the other hand, CLS in the iSAT depot were less pronounced after a high-fat diet, and administration of Cr tepals extract decreased inflammation to the level of control animals. It could be argued that eVAT contributes substantially to obesity-induced insulin resistance, whereas iSAT may play a protective role, and this role is particularly fortified by Cr tepals extract treatment.

Importantly, glucose homeostasis and systemic insulin sensitivity was largely preserved in the Cr tepals extract treated group on HFD. In agreement with our results, other studies also showed positive effects of saffron administration on parameters of insulin sensitivity in metabolic disorders (10). With regard to this restored systemic insulin sensitivity, we further investigated the insulin signaling pathway in the eVAT and iSAT depots locally. In the eVAT depot, the impaired insulin signaling after HFD was confirmed by changes in protein levels

of IRS-1, Akt and GSK3β. On the other hand, insulin signaling was preserved in the iSAT after the HFD. However, the results appear to indicate that Cr tepals extract treatment leads to a slight improvement in the insulin sensitivity of the iSAT depot, due to the detected increase in the ratio between total Akt and its activating phosphorylation. Akt signaling is known to play a central role in insulin-stimulated glucose uptake in both muscle and adipose tissue, and defects in Akt phosphorylation have been associated with the development of insulin resistance in muscle and adipose tissue in obesity (55).

It has been established that the mechanisms controlling the expansion capacity of adipose tissue, including its high capacity for adipocyte differentiation and lipid storage, may be key factors in determining insulin resistance risk in obesity (56). A study using mice fed a high-fat diet showed that VAT developed by hypertrophy, whereas SAT expanded mainly by hyperplasia and had more proliferating adipogenic progenitor cells than VAT (57). Therefore, inhibition of adipogenesis may be an important target for the prevention and treatment of obesity-related complications. Thus, we investigated what effects it might have on adipocyte differentiation and maturation *in vitro*. The results showed that Cr tepals extract significantly decreased the expression profile of the major regulators of adipocyte differentiation and maturation, *Pparγ*, *Cebpa* and *Adipo*, in 3T3-F442A cells. This is in agreement with the previous results obtained with saffron and its active compounds in human adipose tissue-derived stem cells (58) and in 3T3-L1 adipocytes (59, 60). It is noteworthy that *in vitro* testing has its limitations, particularly in light of the fact that the parent compounds undergo metabolic changes *in vivo*, primarily in the gastrointestinal tract, while adipocytes cultured *in vitro* are exposed to the parent compounds. However, *in vitro* studies

can still serve as a valuable screening tool for further investigation if the direct effect of the parent compounds on adipocytes proves desirable. This is of particular importance as the technological advancement of bioactive compounds' administration is rapidly developing. Some of the novel solutions for overcoming the bioavailability problem are the use of nanoparticles (61), liposomes (62), and spray drying for inhalators application of the natural compounds (63), to name a few. In our study, in adipose tissue depots, the level of adipogenic factor PPARɣ was not changed in response to the applied treatments. In both iSAT and eVAT of animals fed a HFD, the expression of *Cebpa* and *Adipo* decreased independently of Cr treatment, whereas tepals extract caused an additional decrease in *Fasn* mRNA levels compared with HFD alone. The expression of the lipogenic enzyme *Pepck* was also reduced in both adipose tissue depots. However, significantly higher *Pepck* mRNA levels were observed only in the eVAT after Cr treatment compared with animals fed only a HFD. This result may explain the observed difference in eVAT and iSAT hypertrophy in Cr-treated obese mice, as upregulation of *Pepck* facilitates lipid storage in adipocytes (64).

So far, *Crocus sativus* stigmas have generally been used in the food, cosmetic and pharmaceutical industries. The results of this study show that another part of the *Crocus sativus* plant, the tepals, which are usually wasted in saffron production, are a source of bioactive compounds with anti-adipogenic potential. Namely, we have demonstrated for the first time that oral ingestion of a Cr tepals extract resulted in weight loss, improved systemic insulin sensitivity, lower triglyceride levels, and improved lipid peroxidation in obese animals. The Cr tepals extract treatment had a suppressive effect on SAT hypertrophy and inhibited differentiation of adipocyte cells *in vitro*. Interestingly, the suppressive effect was

not present in VAT, suggesting that Cr tepals extract treatment has different local effects on adipose tissue development and metabolism, and the possible mechanisms involved need further investigation. With all considered, future pharmaceutical/nutraceutical interventions aimed at improving subcutaneous adipocyte function may help maintain adequate insulin sensitivity and reduce the risk of developing obesity-related complications.

Data Availability Statement: The data that support the findings of this study are available from the corresponding author upon reasonable request.

Funding: This work was supported by the Ministry of Science, Technological Development and Innovation of the Republic of Serbia under Grant No 451-03-47/2023-01/200007 and by ordinary funds of the Polytechnic University of Marche granted to T.B. and E.D. The funders had no role in the design, analysis or writing of this article.

Author contributions: BB: investigation, formal analyses, writing. LB: investigation, formal analyses. MJ: investigation, formal analyses, writing – review and editing. LG: visualization, formal analyses, writing – review and editing. AT: conceptualization, writing – review and editing. MV: formal analyses, writing – review and editing. DVM: writing – review and editing. AA: formal analyses. PMM: formal analyses. CM: formal analyses. ED: conceptualization, writing – review and editing. TB: conceptualization, writing – review and editing. AD: conceptualization, supervision, writing – review and editing. All authors: final approval of the submitted version.

Conflict of interest: The authors declare that they have no conflict of interest.

5. References

[1] Bray, G. A., and Tartaglia, L. A. (2000) Medicinal strategies in the treatment of obesity. *Nature*. **404**, 672–677

[2] Naser, K. A., Gruber, A., and Thomson, G. A. (2006) The emerging pandemic of obesity and diabetes: are we doing enough to prevent a disaster? *Int J Clin Pr.* **60**, 1093–1097

[3] Sun, N. N., Wu, T. Y., and Chau, C. F. (2016) Natural Dietary and Herbal Products in Anti-Obesity Treatment. *Molecules*. 10.3390/molecules21101351

[4] Kang, C., Lee, H., Jung, E. S., Seyedian, R., Jo, M., et al. (2012) Saffron (Crocus sativus L.) increases glucose uptake and insulin sensitivity in muscle cells via multipathway mechanisms. *Food Chem.* **135**, 2350–2358

[5] Milajerdi, A., Jazayeri, S., Hashemzadeh, N., Shirzadi, E., Derakhshan, Z., et al. (2018) The effect of saffron (Crocus sativus L.) hydroalcoholic extract on metabolic control in type 2 diabetes mellitus: A triple-blinded randomized clinical trial. *J Res Med Sci*. **23**, 16

[6] Fang, K., and Gu, M. (2020) Crocin Improves Insulin Sensitivity and Ameliorates Adiposity by Regulating AMPK-CDK5-PPARgamma Signaling. *Biomed Res Int.* **2020**, 9136282

[7] Bathaie, S. Z., and Mousavi, S. Z. (2010) New applications and mechanisms of action of saffron and its important ingredients. *Crit Rev Food Sci Nutr*. **50**, 761–786

[8] Karimi-Nazari, E., Nadjarzadeh, A., Masoumi, R., Marzban, A., Mohajeri, S. A., et al. (2019) Effect of saffron (Crocus sativus L.) on lipid profile, glycemic indices and

antioxidant status among overweight/obese prediabetic individuals: A double-blinded, randomized controlled trial. *Clin Nutr ESPEN*. **34**, 130–136

[9] Azimi, P., Ghiasvand, R., Feizi, A., Hariri, M., and Abbasi, B. (2014) Effects of Cinnamon, Cardamom, Saffron, and Ginger Consumption on Markers of Glycemic Control, Lipid Profile, Oxidative Stress, and Inflammation in Type 2 Diabetes Patients. *Rev Diabet Stud*. **11**, 258–266

[10] Mashmoul, M., Azlan, A., Khaza'ai, H., Yusof, B. N., and Noor, S. M. (2013) Saffron: A Natural Potent Antioxidant as a Promising Anti-Obesity Drug. *Antioxidants (Basel)*. **2**, 293–308

[11] Hosseini, A., Razavi, B. M., and Hosseinzadeh, H. (2018) Saffron (Crocus sativus) petal as a new pharmacological target: a review. *Iran J Basic Med Sci*. **21**, 1091–1099

[12] Bellachioma, L., Morresi, C., Albacete, A., Martinez-Melgarejo, P. A., Ferretti, G., et al. (2023) Insights on the Hypoglycemic Potential of Crocus sativus Tepal Polyphenols: An In Vitro and In Silico Study. *Int J Mol Sci*. 10.3390/ijms24119213

[13] Hoshyar R Bathaie S., M. S. (2016) Anticancer effects of saffron stigma (Crocus Sativus). *RJMS*. **22**, 69–78

[14] Saponaro, C., Gaggini, M., Carli, F., and Gastaldelli, A. (2015) The Subtle Balance between Lipolysis and Lipogenesis: A Critical Point in Metabolic Homeostasis. *Nutrients*. **7**, 9453–9474

[15] Gao, H., Volat, F., Sandhow, L., Galitzky, J., Nguyen, T., et al. (2017) CD36 Is a Marker of Human Adipocyte Progenitors with Pronounced Adipogenic and Triglyceride Accumulation Potential. *Stem Cells*. **35**, 1799–1814

[16] Rosen, E. D., Walkey, C. J., Puigserver, P., and Spiegelman, B. M. (2000)

Transcriptional regulation of adipogenesis. *Genes Dev*. **14**, 1293–1307

[17] Madsen, M. S., Siersbaek, R., Boergesen, M., Nielsen, R., and Mandrup, S. (2014) Peroxisome proliferator-activated receptor gamma and C/EBPalpha synergistically activate key metabolic adipocyte genes by assisted loading. *Mol Cell Biol*. **34**, 939–954

[18] Wajchenberg, B. L. (2000) Subcutaneous and visceral adipose tissue: their relation to the metabolic syndrome. *Endocr. Rev*. **21**, 697–738

[19] Danforth Jr., E. (2000) Failure of adipocyte differentiation causes type II diabetes mellitus? *Nat Genet*. **26**, 13

[20] Smith, G. I., Mittendorfer, B., and Klein, S. (2019) Metabolically healthy obesity: facts and fantasies. *J. Clin. Invest.* **129**, 3978

[21] Smith, U., and Kahn, B. B. (2016) Adipose tissue regulates insulin sensitivity: role of adipogenesis, de novo lipogenesis and novel lipids. *J Intern Med*. **280**, 465–475

[22] Boucher, J., Kleinridders, A., and Kahn, C. R. (2014) Insulin receptor signaling in normal and insulin-resistant states. *Cold Spring Harb Perspect Biol*. 10.1101/cshperspect.a009191

[23] Kanda, H., Tateya, S., Tamori, Y., Kotani, K., Hiasa, K., et al. (2006) MCP-1 contributes to macrophage infiltration into adipose tissue, insulin resistance, and hepatic steatosis in obesity. *J Clin Invest*. **116**, 1494–1505

[24] Sani, A., Tajik, A., Seiiedi, S. S., Khadem, R., Tootooni, H., et al. (2022) A review of the anti-diabetic potential of saffron. *Nutr Metab Insights*. **15**, 11786388221095224

[25] Konstantopoulos, P., Doulamis, I., Tzani, A., Korou, M.-L., Agapitos, E., et al. (2017) Metabolic effects of Crocus sativus and protective action against non-alcoholic fatty

liver disease in diabetic rats. *Biomed. Reports*. **6**, 513

[26] Karimi-Nazari, E., Nadjarzadeh, A., Masoumi, R., Marzban, A., Mohajeri, S. A., et al. (2019) Effect of saffron (Crocus sativus L.) on lipid profile, glycemic indices and antioxidant status among overweight/obese prediabetic individuals: A double-blinded, randomized controlled trial. *Clin. Nutr. ESPEN*. **34**, 130–136

[27] Sabir Ouahhoud Mohamed Bouhrim, Amine Khoulati, Assia Sabouni, Redouanae, I. L., Iliass Lahmass Amine Khoulati, Assia Sabouni, Redouanae Benabbes, M. B., and Abdeslam Asehraou Mohamed Bnouham, Ennouamane Saalaoui., M. C. (2019) Antidiabetic effect of hydroethanolic extract of Crocus sativus. stigmas, tepals and leaves instreptozotocin-induced diabetic rats. *Physiol Pharmacol*. **23**, 9–20

[28] Ouahhoud, S., Lahmass, I., Bouhrim, M., Khoulati, A., Sabouni, A., et al. (2019) Antidiabetic effect of hydroethanolic extract of Crocus sativus stigmas, tepals and leaves in streptozotocin-induced diabetic rats. *Physiol. Pharmacol.* **23**, 9–20

[29] Ouahhoud, S., Bencheikh, N., Khoulati, A., Kadda, S., Mamri, S., et al. (2022) Crocus sativus L. Stigmas, Tepals, and Leaves Ameliorate Gentamicin-Induced Renal Toxicity: A Biochemical and Histopathological Study. *Evidence-based Complement. Altern. Med.* 10.1155/2022/7127037

[30] Hosseinzadeh, H., and Younesi, H. M. (2002) Antinociceptive and anti-inflammatory effects of Crocus sativus L. stigma and petal extracts in mice. *BMC Pharmacol.* **2**, 7

[31] Babaei, A., Arshami, J., Haghparast, A., and Danesh Mesgaran, M. (2014) Effects of saffron (Crocus sativus) petal ethanolic extract on hematology, antibody response, and spleen histology in rats. *Avicenna J. phytomedicine*. **4**, 103–9

[32] Reagan-Shaw, S., Nihal, M., and Ahmad, N. (2008) Dose translation from animal to

human studies revisited. *FASEB J.* **22**, 659–661

[33] Bae, J. W., Kim, D. H., Lee, W. W., Kim, H. Y., and Son, C. G. (2015) Characterizing the human equivalent dose of herbal medicines in animal toxicity studies. *J. Ethnopharmacol.* **162**, 1–6

[34] Leopoldo, A. S., Lima-Leopoldo, A. P., Nascimento, A. F., Luvizotto, R. A., Sugizaki, M. M., et al. (2016) Classification of different degrees of adiposity in sedentary rats. *Braz J Med Biol Res*. **49**, e5028

[35] van Beek, L., van Klinken, J. B., Pronk, A. C., van Dam, A. D., Dirven, E., et al. (2015) The limited storage capacity of gonadal adipose tissue directs the development of metabolic disorders in male C57Bl/6J mice. *Diabetologia*. **58**, 1601–1609

[36] Misra, A., Garg, A., Abate, N., Peshock, R. M., Stray-Gundersen, J., et al. (1997) Relationship of anterior and posterior subcutaneous abdominal fat to insulin sensitivity in nondiabetic men. *Obes Res*. **5**, 93–99

[37] Fryklund, C., Neuhaus, M., Moren, B., Borreguero-Munoz, A., Lundmark, R., et al. (2022) Expansion of the Inguinal Adipose Tissue Depot Correlates With Systemic Insulin Resistance in C57BL/6J Mice. *Front Cell Dev Biol*. **10**, 942374

[38] Galarraga, M., Campión, J., Munõz-Barrutia, A., Boqué, N., Moreno, H., et al. (2012) Adiposoft: Automated software for the analysis of white adipose tissue cellularity in histological sections. *J. Lipid Res.* **53**, 2791–2796

[39] Berry, R., Church, C. D., Gericke, M. T., Jeffery, E., Colman, L., et al. (2014) Imaging of adipose tissue. in *Methods in Enzymology*, pp. 47–73, Academic Press, **537**, 47–73

[40] Camastra, S., Vitali, A., Anselmino, M., Gastaldelli, A., Bellini, R., et al. (2017) Muscle and adipose tissue morphology, insulin sensitivity and beta-cell function in

diabetic and nondiabetic obese patients: effects of bariatric surgery. *Sci Rep*. **7**, 9007

[41] Livak, K. J., and Schmittgen, T. D. (2001) Analysis of relative gene expression data using real-time quantitative PCR and the 2-ΔΔCT method. *Methods*. **25**, 402–408

[42] Lowry, O. H., Rosebrough, N. J., Farr, A. L., and Randall, R. J. (1951) Protein measurement with the Folin phenol reagent. *J. Biol. Chem.* **193**, 265–275

[43] Lee, S. (2018) Current knowledge for the western blot normalization. *J Med Oncl Ther*. **3**, 3–9

[44] Bellachioma, L., Marini, E., Magi, G., Pugnaloni, A., Facinelli, B., et al. (2022) Phytochemical profiling, antibacterial and antioxidant properties of Crocus sativus flower: A comparison between tepals and stigmas. *Open Chem.* **20**, 431–443

[45] Stelluti, S., Caser, M., Demasi, S., and Scariot, V. (2021) Sustainable processing of floral bio-residues of saffron (Crocus sativus l.) for valuable biorefinery products. *Plants*. **10**, 1–15

[46] M. Mashmoul B. N. M. Yusof, H. Khaza'ai, N. Mohtarrudin, and M. T. Boroushaki, A. A. (2014) Effects of saffron extract and crocin on anthropometrical, nutritional and lipid profile parameters of rats fed a high fat diet,. *J. Funct. Foods*. **8**, 180–187

[47] Mohaqiq, Z., Moossavi, M., Hemmati, M., Kazemi, T., and Mehrpour, O. (2020) Antioxidant Properties of Saffron Stigma and Petals: A Potential Therapeutic Approach for Insulin Resistance through an Insulin-Sensitizing Adipocytokine in High-Calorie Diet Rats. *Int J Prev Med*. **11**, 184

[48] Bellachioma, L., Rocchetti, G., Morresi, C., Martinelli, E., Lucini, L., et al. (2022) Valorisation of Crocus sativus flower parts for herbal infusions: impact of brewing conditions on phenolic profiling, antioxidant capacity and sensory traits. *Int. J. Food*

Sci. Technol. **57**, 3838–3849

[49] Patel, P., and Abate, N. (2013) Body fat distribution and insulin resistance. *Nutrients*. **5**, 2019–2027

[50] Andersson, D. P., Eriksson Hogling, D., Thorell, A., Toft, E., Qvisth, V., et al. (2014) Changes in subcutaneous fat cell volume and insulin sensitivity after weight loss. *Diabetes Care*. **37**, 1831–1836

[51] Hajri, T., Han, X. X., Bonen, A., and Abumrad, N. A. (2002) Defective fatty acid uptake modulates insulin responsiveness and metabolic responses to diet in CD36-null mice. *J Clin Invest*. **109**, 1381–1389

[52] Bonen, A., Tandon, N. N., Glatz, J. F., Luiken, J. J., and Heigenhauser, G. J. (2006) The fatty acid transporter FAT/CD36 is upregulated in subcutaneous and visceral adipose tissues in human obesity and type 2 diabetes. *Int J Obes*. **30**, 877–883

[53] Zatterale, F., Longo, M., Naderi, J., Raciti, G. A., Desiderio, A., et al. (2019) Chronic Adipose Tissue Inflammation Linking Obesity to Insulin Resistance and Type 2 Diabetes. *Front Physiol*. **10**, 1607

[54] Honecker, J., Ruschke, S., Seeliger, C., Laber, S., Strobel, S., et al. (2022) Transcriptome and fatty-acid signatures of adipocyte hypertrophy and its non-invasive MR-based characterization in human adipose tissue. *EBioMedicine*. **79**, 104020

[55] Steinberg, G. R., and Kemp, B. E. (2009) AMPK in Health and Disease. *Physiol Rev*. **89**, 1025–1078

[56] Hardy, O. T., Czech, M. P., and Corvera, S. (2012) What causes the insulin resistance underlying obesity? *Curr Opin Endocrinol Diabetes Obes*. **19**, 81–87

[57] Joe, A. W., Yi, L., Even, Y., Vogl, A. W., and Rossi, F. M. (2009) Depot-specific

differences in adipogenic progenitor abundance and proliferative response to high-fat diet. *Stem Cells*. **27**, 2563–2570

[58] Jafari, F., Emami, S. A., Javadi, B., Salmasi, Z., Tayarani-Najjaran, M., et al. (2022) Inhibitory effect of saffron, crocin, crocetin, and safranal against adipocyte differentiation in human adipose-derived stem cells. *J Ethnopharmacol*. **294**, 115340

[59] Cimas, F. J., De la Cruz-Morcillo, M. A., Cifuentes, C., Moratalla-Lopez, N., Alonso, G. L., et al. (2023) Effect of Crocetin on Basal Lipolysis in 3T3-L1 Adipocytes. *Antioxidants (Basel)*. 10.3390/antiox12061254

[60] Min, B., Lee, H., Song, J. H., Han, M. J., and Chung, J. (2014) Arctiin inhibits adipogenesis in 3T3-L1 cells and decreases adiposity and body weight in mice fed a high-fat diet. *Nutr Res Pr.* **8**, 655–661

[61] Gómez-Guillén, M. C., and Montero, M. P. (2021) Enhancement of oral bioavailability of natural compounds and probiotics by mucoadhesive tailored biopolymer-based nanoparticles: A review. *Food Hydrocoll.* **118**, 106772

[62] Tan, O. J., Loo, H. L., Thiagarajah, G., Palanisamy, U. D., and Sundralingam, U. (2021) Improving oral bioavailability of medicinal herbal compounds through lipid-based formulations – A Scoping Review. *Phytomedicine*. **90**, 153651

[63] Wang, B., Xiang, J., He, B., Tan, S., and Zhou, W. (2023) Enhancing bioavailability of natural extracts for nutritional applications through dry powder inhalers (DPI) spray drying: technological advancements and future directions. *Front. Nutr.* **10**, 1190912

[64] Tordjman, J., Khazen, W., Antoine, B., Chauvet, G., Quette, J., et al. (2003) Regulation of glyceroneogenesis and phosphoenolpyruvate carboxykinase by fatty acids, retinoic acids and thiazolidinediones: Potential relevance to type 2 diabetes. in

Biochimie, pp. 1213–1218, Elsevier, **85**, 1213–1218

Figure captions

Figure 1

Histological and morphometric analysis of epididymal VAT (eVAT) (**A**) and inguinal SAT (iSAT) (**B**) in control group (C), high-fat diet group (HFD) and high-fat diet + Cr tepals extract group (HFD+Cr). Representative sections of eVAT and iSAT are shown in Figure **A1** and **B1**, respectively (magnification ×20, bar = 100 μm). Morphometric data on eVAT adipocyte cell diameter (**A2**), area (**A3**) and adipocyte size distribution (**A4**), as well as iSAT adipocyte cell diameter (**B2**), area (**B3**) and adipocyte size distribution (**B4**) are presented as mean ± SEM (100 adipocytes per section, 3 sections per animal and 5 animals per group). CLS number was determined as total number of CLSs per group (3 sections per animal and 5 animals per group). A one-way ANOVA followed by the Tukey *post hoc* test or non-parametric Kruskal–Wallis *H* test followed by *post hoc* Dunn's test were performed. Different superscripts signify significant mean differences. The difference was considered significant at $P<0.05$.

Figure 2

Intraperitoneal glucose tolerance test (ipGTT) in control group (C), high-fat diet group (HFD) and high-fat diet + Cr tepals extract group (HFD+Cr). All data are presented as mean ± SEM (n = 9-11 animals per group). At each time point a one-way ANOVA followed by the Tukey *post hoc* test was performed, and the difference was considered significant at $P<0.05$. Different superscripts signify significant mean differences.

Figure 3

Insulin signaling in the epididymal VAT (eVAT) (**A**) and inguinal SAT (iSAT) (**B**) in control group (C), high-fat diet group (HFD) and high-fat diet + Cr tepals extract (HFD+Cr). (**A1** and **B1**). Protein levels of pIRS1^{Ser307}, IRS1 and their relative ratio with representative Western blots in the eVAT and iSAT depots, respectively. (**A2** and **B2**) Protein levels of pAkt^{Thr308}, Akt and their relative ratio with representative Western blots in the eVAT and iSAT depots, respectively. (**3A** and **B3**) Protein levels of pGSK3β^{Ser9}, GSK3α/β and their relative ratio with representative Western blots in the eVAT and iSAT depots, respectively. All protein levels were measured in the total protein extract of eVAT and iSAT and normalized to calnexin. The data are presented as mean ± SEM (n = 5-9 animals per group). One-way ANOVA followed by the Tukey *post hoc* test or non-parametric Kruskal–Wallis *H* test followed by *post hoc* Dunn's test were performed. The difference was considered significant at $P<0.05$. Different superscripts signify significant mean differences.

Figure 4

The effects of Cr tepals extract on 3T3-F442A differentiation. The cells were treated with 25 or 100 μg/mL of tepals extract for 5 days (days 9th to 14th of differentiation), or during the whole 14 days of differentiation. Mean values ± SD were obtained from four independent experiments. Data were analyzed by unpaired t test with Welch's correction, and the difference was considered significant at $P<0.05$. Different superscripts signify significant mean differences.

Figure 5

The levels of proteins involved in adipose tissue lipo/adipogenesis, SREBP1C, PPARγ and perilipin-2, with representative Western blots in the epididymal VAT (eVAT) (**A1**) and inguinal SAT (iSAT) (**B1**) in control group (C), high-fat diet group (HFD) and high-fat diet + Cr tepals extract group (HFD+Cr). All protein levels were measured in the total protein extract of eVAT and iSAT depots and normalized to calnexin. The data are presented as mean ± SEM (n = 6-9 animals per group). One-way ANOVA followed by the Tukey *post hoc* test or non-parametric Kruskal–Wallis *H* test followed by *post hoc* Dunn's test were performed. The difference was considered significant at $P<0.05$. Different superscripts signify significant mean differences.

Figure 6

Proteins involved in fatty acid transport, CD36 and FATP4, in the epididymal VAT (eVAT) (**A1**) and inguinal SAT (iSAT) (**B1**) in control group (C), high-fat diet group (HFD) and high-fat diet + Cr tepals extract group (HFD+Cr). All protein levels were measured in the total protein extract of VAT and SAT depots and normalized to calnexin. The data are presented as mean ± SEM (n = 6-9 animals per group). One-way ANOVA followed by the Tukey *post hoc* test or non-parametric Kruskal–Wallis *H* test followed by *post hoc* Dunn's test were performed. The difference was considered significant at $P<0.05$. Different superscripts signify significant mean differences.

Figure 7

Relative expression of markers of lipolysis (*Hsl*, *Lpl*, *Atgl*) and adipo/lipogenesis (*Fasn*, *Pepck*, *Adipo* and *Cebpa*) in the epididymal VAT (eVAT) (**A1** and **A2**, respectively) and inguinal SAT (iSAT) (**B1** and **B2**, respectively) in control group (C), high-fat diet group (HFD) and high-fat diet + Cr tepals extract group (HFD+Cr). The gene expression was normalized to *Hprt* and the data are presented as mean ± SEM (n = 9 animals per group). One-way ANOVA followed by the Tukey *post hoc* test or non-parametric Kruskal–Wallis *H* test followed by *post hoc* Dunn's test were performed. The difference was considered significant at $P<0.05$. Different superscripts signify significant mean differences.

Table 1. The effects of high-fat diet and *Crocus sativus* tepals extract on morphological parameters

	C	HFD	HFD+Cr
Caloric intake (kcal /day/animal)	9.19 ± 0.4	14.48 ± 0.32 ***	15.37 ± 0.48 ***
Body mass (g)	34.00 ± 0.94	46.88 ± 1.53 ***	41.38 ± 1.97 **#
eVAT mass (g)	1.25 ± 0.15	2.32 ± 0.14 ***	2.50 ± 0.11 ***
iSAT mass (g)	0.93 ± 0.11	2.76 ± 0.19 ***	2.03 ± 0.24 ***#
Adiposity Index (AI) (%)	5.45 ± 0.51	9.28 ± 0.60 **	9.19 ± 0.50 **

All data are presented as mean ± SEM (n = 9-11 animals per group). Food intake, energy intake, body mass, epididymal visceral adipose tissue (eVAT) mass, inguinal subcutaneous adipose tissue (iSAT) mass and index of adiposity (AI) were measured in control group (C), high-fat diet group (HFD) and high-fat diet + *Crocus sativus* tepals extract group (HFD+Cr). To determine the effects of high-fat diet and *Crocus sativus* treatment, a one-way ANOVA followed by the Tukey *post hoc* test or non-parametric Kruskal–Wallis *H* test followed by *post hoc* Dunn's test were performed. The difference was considered significant at $p<0.05$. Asterisk indicates a significant difference between control group and high-fat diet group (HFD *vs.* C, **$p<0.01$, ***$p<0.001$) or control group and high-fat diet + *Crocus sativus* tepals extract group (HFD+Cr *vs.* C, **$p<0.01$, ***$p<0.001$), hashtag indicates a significant difference between high-fat diet group and high-fat diet + *Crocus sativus* tepals extract group (HFD+Cr *vs.* HFD, $^{\#}p<0.05$).

Table 2. The effects of high fat diet and *Crocus sativus* tepals extract on systemic insulin sensitivity parameters, triglycerides and MDA level

	C	HFD	HFD+Cr
Glucose (mmol/L))	9.27 ± 0.64	12.76 ± 0.65***	10.09 ± 0.25
Insulin (mIU /mL)	2.55 ± 0.35	6.87 ± 1.36 *	4.38 ± 0.91
HOMA index	0.37 ± 0.07	1.23 ± 0.26 **	0.71 ± 0.21
Triglycerides (mmol/L)	2.1 ± 0 .12	1.94 ± 0.14	1.55 ± 0.15*
MDA (nmol/ml)	13.21 ± 0.41	13.58 ± 0.45	11.95 ± 0.61**##

All data are presented as mean ± SEM (n = 9-11 animals per group). Glucose level, insulin level, HOMA index and MDA level were measured in control group (C), high-fat diet group (HFD) and high-fat diet + *Crocus sativus* tepals extract group (HFD+Cr). To determine the effects of high-fat diet and *Crocus sativus* treatment, a one-way ANOVA followed by the Tukey *post hoc* test or non-parametric Kruskal–Wallis *H* test followed by *post hoc* Dunn's test were performed. The difference was considered significant at $p<0.05$. Asterisk indicates a significant difference between control group and high-fat diet group (C *vs.* HFD, *$p<0.05$, **$p<0.01$, ***$p<0.001$) or control group and high-fat diet + *Crocus sativus* tepals extract group (C *vs.* HFD+Cr, *$p<0.05$, **$p<0.01$), hashtag indicates a significant difference between high-fat diet group and high-fat diet + *Crocus sativus* tepals extract group (HFD *vs.* HFD+Cr, $^{\#\#}p<0.01$).

Figure 1

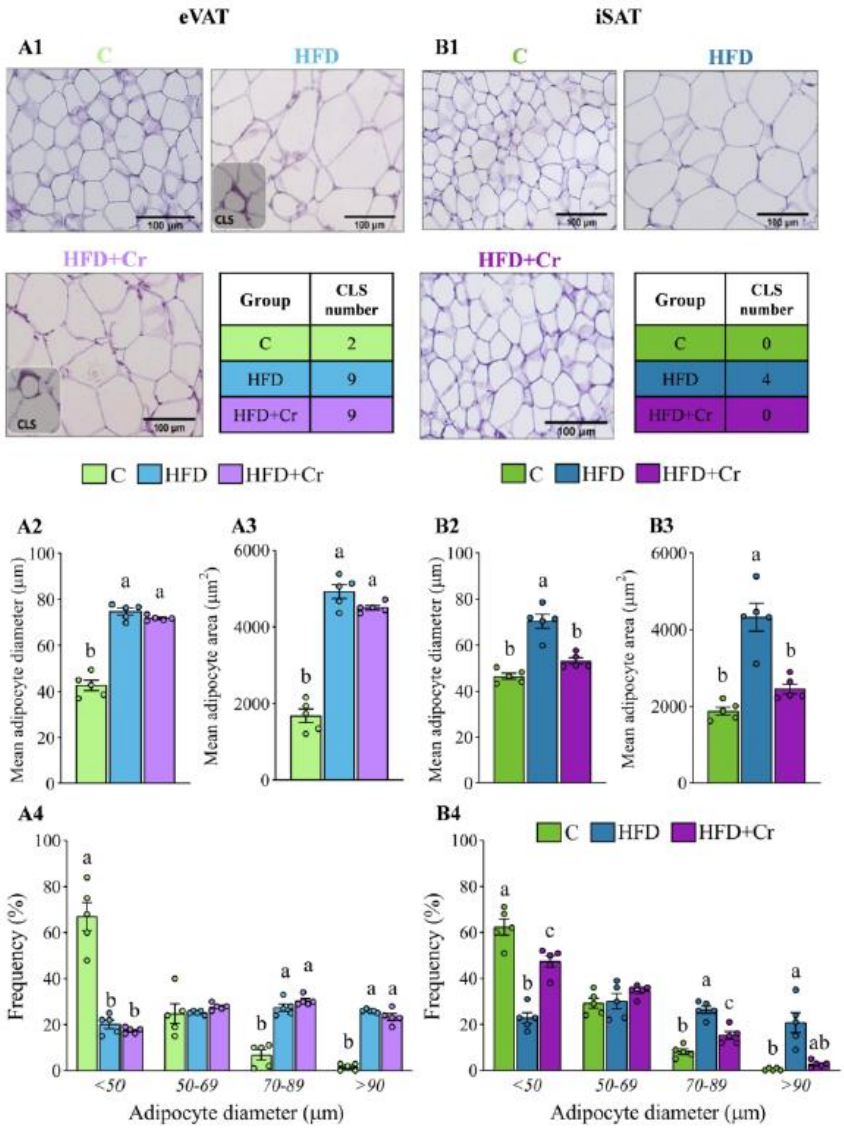
eVAT
iSAT
A1
B1
C
HFD
HFD+Cr
CLS
100 μm
Group
CLS number
C 2
HFD 9
HFD+Cr 9
C 0
HFD 4
HFD+Cr 0
C HFD HFD+Cr
A2
A3
B2
B3
Mean adipocyte diameter (μm)
Mean adipocyte area (μm²)
A4
B4
Frequency (%)
<50
50-69
70-89
>90
Adipocyte diameter (μm)

Figure 2

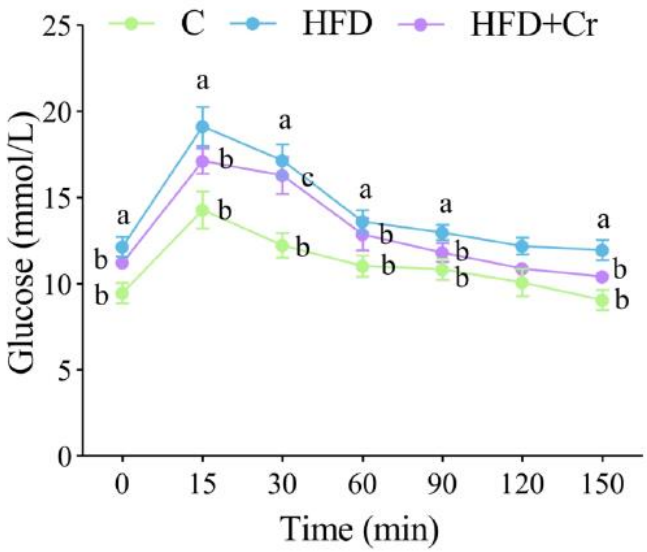
C
HFD
HFD+Cr
Glucose (mmol/L)
Time (min)
25
20
15
10
5
0
0
15
30
60
90
120
150
a
b
a
b
c
a
b
a
b
a
b
b
b
b
b
b
b
b
b

Figure 3

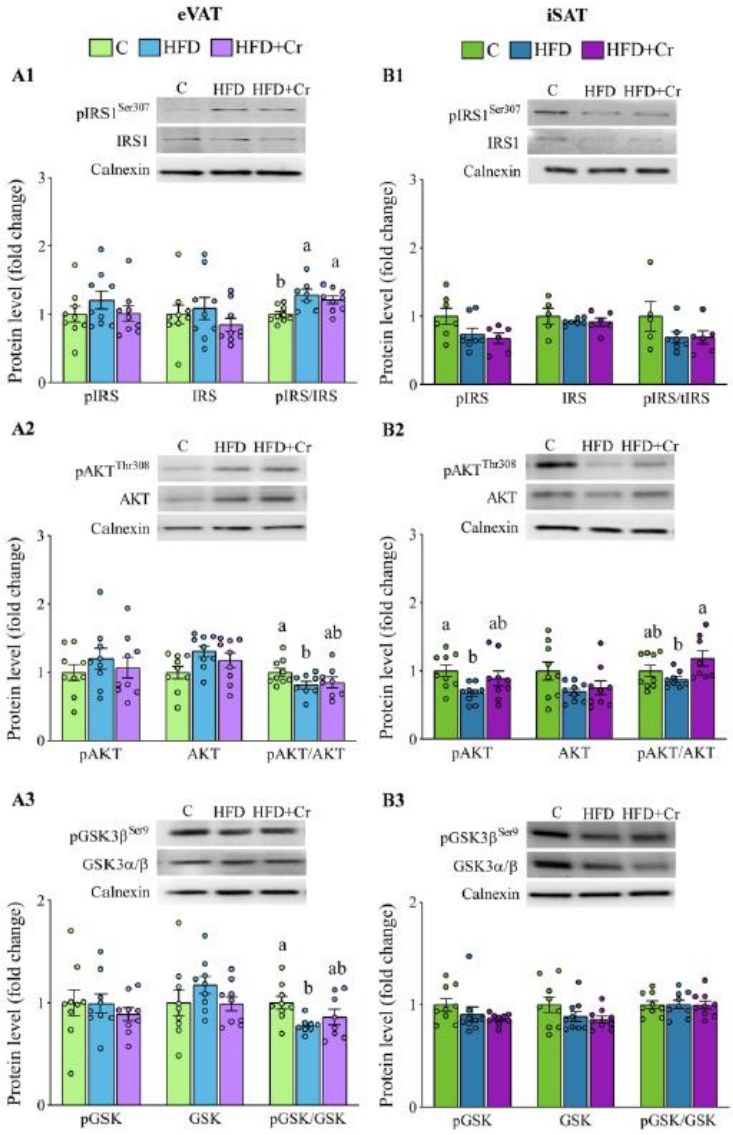
eVAT
iSAT
C HFD HFD+Cr
A1
B1
pIRS1Ser307
IRS1
Calnexin
Protein level (fold change)
pIRS
IRS
pIRS/IRS
pIRS/tIRS
A2
B2
pAKTThr308
AKT
pAKT
pAKT/AKT
A3
B3
pGSK3βSer9
GSK3α/β
pGSK
GSK
pGSK/GSK

Figure 4

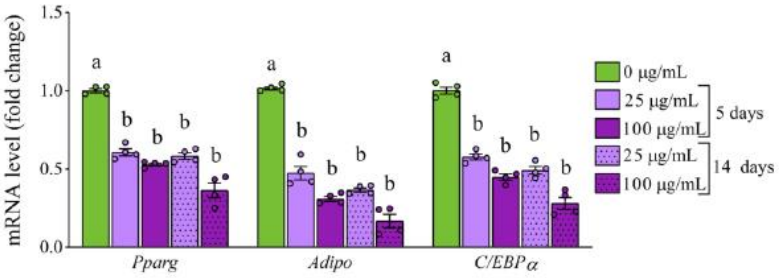
mRNA level (fold change)
1.5
1.0
0.5
0.0
a
b
b
b
b
a
b
b
b
b
a
b
b
b
b
Pparg
Adipo
C/EBPα
0 μg/mL
25 μg/mL
100 μg/mL
5 days
25 μg/mL
100 μg/mL
14 days

Figure 5

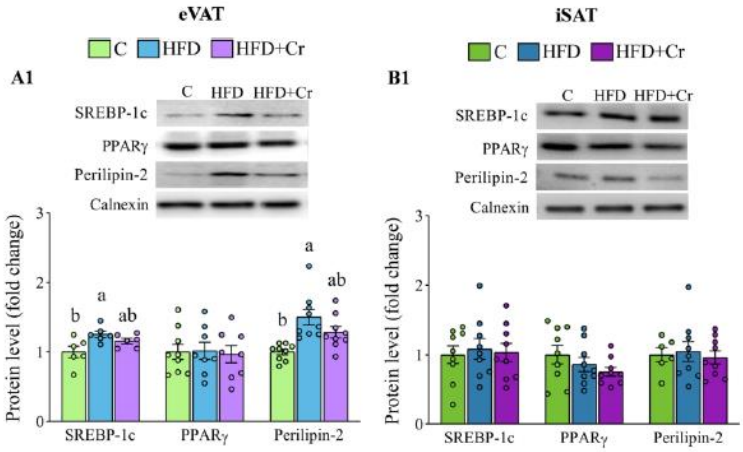
eVAT
C HFD HFD+Cr
A1
C HFD HFD+Cr
SREBP-1c
PPARγ
Perilipin-2
Calnexin
Protein level (fold change)
SREBP-1c
PPARγ
Perilipin-2
iSAT
C HFD HFD+Cr
B1
C HFD HFD+Cr
SREBP-1c
PPARγ
Perilipin-2
Calnexin
Protein level (fold change)
SREBP-1c
PPARγ
Perilipin-2

Figure 6

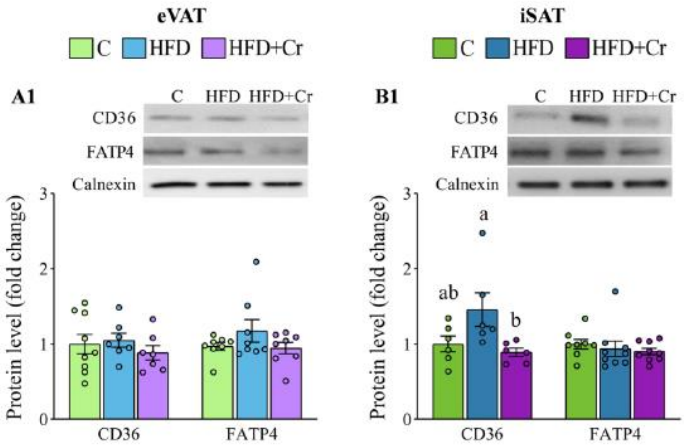
eVAT
C HFD HFD+Cr
A1
C HFD HFD+Cr
CD36
FATP4
Calnexin
Protein level (fold change)
0
1
2
3
CD36
FATP4
iSAT
C HFD HFD+Cr
B1
C HFD HFD+Cr
CD36
FATP4
Calnexin
a
ab
b
Protein level (fold change)
0
1
2
3
CD36
FATP4

Figure 7

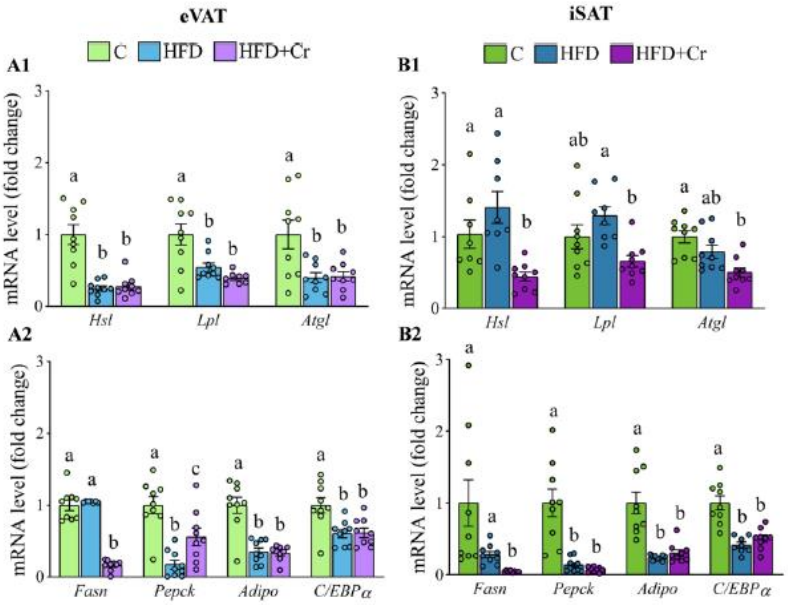
eVAT
iSAT
C
HFD
HFD+Cr
A1
B1
A2
B2
mRNA level (fold change)
Hsl
Lpl
Atgl
Fasn
Pepck
Adipo
C/EBPα

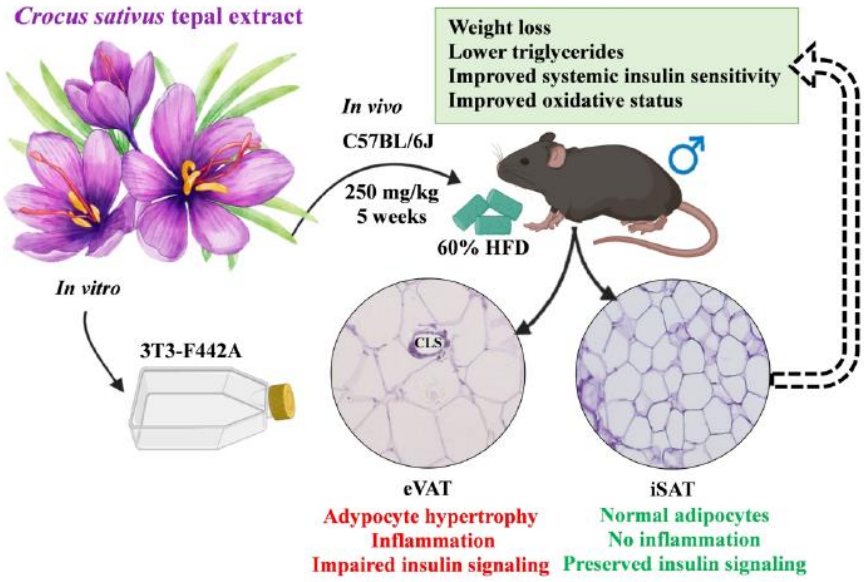

Graphical Abstract